Charge Transfer in the K Proton Pathway Linked to Electron Transfer to the Catalytic Site in Cytochrome *c* Oxidase

Håkan Lepp, Emelie Svahn, Kristina Faxén,‡ and Peter Brzezinski*

Department of Biochemistry and Biophysics, The Arrhenius Laboratories for Natural Sciences, Stockholm University, SE-106 91 Stockholm, Sweden

Received December 19, 2007; Revised Manuscript Received February 6, 2008

ABSTRACT: Cytochrome *c* oxidase couples electron transfer from cytochrome *c* to O_2 to proton pumping across the membrane. In the initial part of the reaction of the reduced cytochrome *c* oxidase with O_2, an electron is transferred from heme *a* to the catalytic site, parallel to the membrane surface. Even though this electron transfer is not linked to proton uptake from solution, recently Belevich et al. [(2006) *Nature 440*, 829] showed that it is linked to transfer of charge perpendicular to the membrane surface (electrogenic reaction). This electrogenic reaction was attributed to internal transfer of a proton from Glu286, in the D proton pathway, to an unidentified protonatable site "above" the heme groups. The proton transfer was proposed to initiate the sequence of events leading to proton pumping. In this study, we have investigated electrogenic reactions in structural variants of cytochrome *c* oxidase in which residues in the second, K proton pathway of cytochrome *c* oxidase were modified. The results indicate that the electrogenic reaction linked to electron transfer to the catalytic site originates from charge transfer within the K pathway, which presumably facilitates reduction of the site.

Energy conservation in aerobic organisms involves transfer of electrons through a number of membrane-bound enzyme complexes of the respiratory chain where cytochrome *c* oxidase (Cyt*c*O)[1] is the final component. The enzyme receives electrons from cytochrome *c* and catalyzes the four-electron reduction of molecular oxygen to water. Protons are taken from the more negative side of the membrane (N-side), and electrons are donated from the more positive side (P-side). In addition, part of the free energy released in this exergonic reaction is used to translocate four protons from the N-side to the P-side across the membrane, resulting in charge separation of eight charge equivalents across the membrane for each O_2 molecule reduced to H_2O:

$$8H_N + 4e_P + O_2 \rightarrow 2H_2O + 4H_P$$

where the subscripts N and P refer to the N- and P-sides of the membrane, respectively. The transmembrane charge separation contributes to the maintenance of an electrochemical proton gradient that is used, for example, for production of ATP.

The Cyt*c*O from *Rhodobacter sphaeroides* binds four redox-active metal centers (*1, 2*): Cu_A, heme *a*, heme a_3, and Cu_B (Figure 1a), the two latter of which make up the catalytic site where molecular oxygen is bound and reduced to water. During Cyt*c*O turnover, electrons are delivered one by one from cytochrome *c* to Cu_A and are then transferred consecutively to heme *a* and the catalytic site. Protons are transferred through two proton transfer pathways denoted by the letters D and K (after the highly conserved residues D132 and K362, respectively), composed of polar residues and water molecules (Figure 1a). The D pathway starts at aspartic acid D132 and leads to the highly conserved glutamic acid residue E286, from where protons are transferred either to the catalytic site or to an acceptor for protons that are pumped. In *R. sphaeroides* Cyt*c*O, the K pathway presumably starts at E101 in subunit II and leads to the catalytic site via the conserved K362. The K pathway is used to transfer one or two protons toward the catalytic site during its reduction, while the D pathway is used to transfer the remaining six or seven protons. Thus, the D pathway transfers both substrate protons and protons that are pumped across the membrane, where the branching point is presumably located at E286 (see Figure 1a). The exit route for the pumped protons is not known, but one candidate is the Δ-propionate of heme a_3, which has been proposed to act as an acceptor for protons transferred from E286 (for recent reviews on the structure and function of Cyt*c*O, see refs *3–11*).

The reaction of the fully reduced Cyt*c*O with O_2 is conveniently studied using the flow-flash technique. When this technique is used, the enzyme with CO bound at heme a_3 is mixed with an O_2-containing solution after which the CO ligand is dissociated by a short laser flash (the resulting

* To whom correspondence should be addressed. Fax: (+46)-8-153679. Phone: (+46)-8-163280. E-mail: peterb@dbb.su.se.

‡ Present address: The Centre for Structural Biology, Department of Molecular Biology, University of Aarhus, Science Park, Gustav Wieds Vej 10c, DK-8000 Århus C, Denmark.

[1] Abbreviations: Cyt*c*O, cytochrome *c* oxidase; SUV, small unilamellar vesicle; R^2, Cyt*c*O with a two-electron reduced catalytic site (the superscript indicates the number of electrons at the catalytic site); P^3 (also P_R), "peroxy" intermediate formed at the catalytic site upon reaction of the four-electron reduced Cyt*c*O with O_2; F^3, "oxo−ferryl" intermediate; O^0 or O^4, fully oxidized Cyt*c*O; N-side, negative side of the membrane; P-side, positive side of the membrane. Time constants are given as (rate constant)$^{-1}$. Unless indicated otherwise, the amino acid residue numbering refers to the *Rhodobacter sphaeroides* cytochrome aa_3 sequence of subunit I.

10.1021/bi7024707 CCC: $40.75
Published on Web 04/05/2008

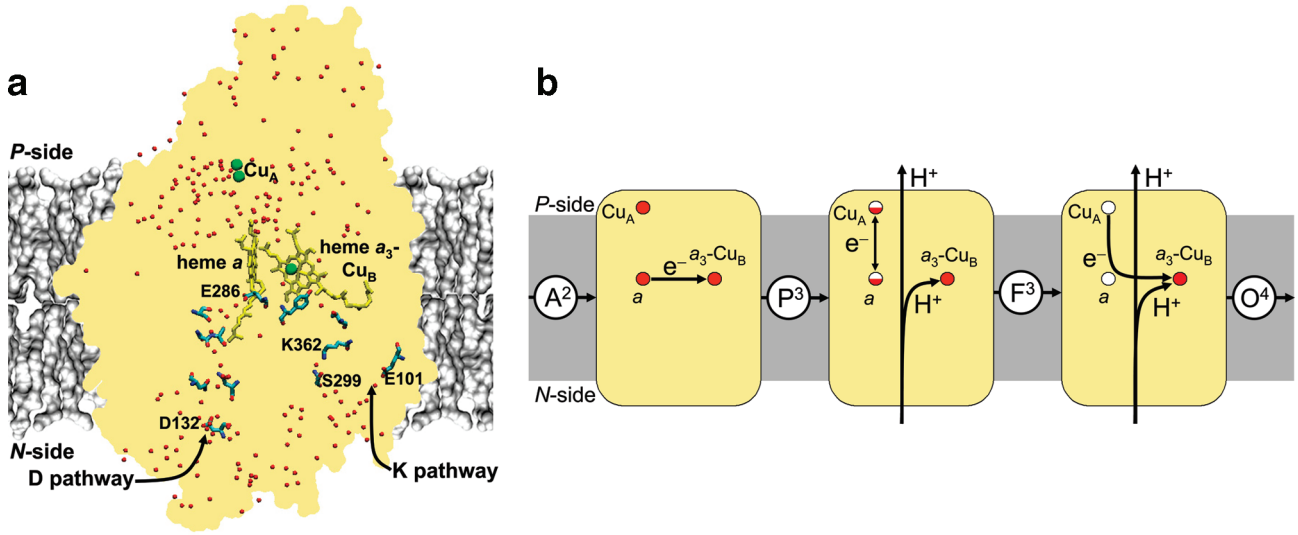

FIGURE 1: (a) Structure of Cyt*c*O and its approximate position in the membrane. The profile of the enzyme is illustrated in light yellow, with the four redox-active metal sites, and selected residues along the two proposed proton transfer pathways (*R. sphaeroides* Cyt*c*O, Protein Data Bank entry 1M56): the D and K pathways (E101 is found in subunit II, while the remaining residues shown in the picture are in subunit I). Hemes *a* and a_3 are colored yellow. The green spheres are copper ions, and the red spheres are water molecules. The figure was prepared using Visual Molecular Dynamics (*54*). (b) Reaction sequence after binding of O_2 to the four-electron reduced Cyt*c*O. First, the A^2 state is formed in which O_2 is bound to reduced heme a_3. In the next step, an electron is transferred from heme *a* to the catalytic site forming state P^3. In each of the $P^3 \rightarrow F^3$ and $F^3 \rightarrow O^4$ transitions, a proton is taken up from solution to the catalytic site and one proton is pumped across the membrane. During these transitions, the electron initially residing at Cu_A first equilibrates with heme *a* and then is transferred to the catalytic site. The filled and empty circles represent reduced and oxidized redox sites (the half-filled circles illustrate the electron equilibration between Cu_A and heme *a*), respectively.

state is denoted R^2, where the superscript refers to the number of electrons at the catalytic site). The reaction of the fully reduced *R. sphaeroides* Cyt*c*O with O_2 is described in more detail in ref *12* and reviewed, for example, in refs *5* and *13–16*. Briefly, when the blocking CO ligand is removed, O_2 binds to reduced heme a_3 with a time constant of ~10 μs (at 1 mM O_2) forming a state called A^2. If initially all four redox sites are reduced (i.e., heme *a* and Cu_A are reduced in addition to the catalytic site), in the next step an electron is transferred from heme *a* to the catalytic site forming the "peroxy" state called P^3 with a time constant of ~30 μs at pH 7.5 (Figure 1b). The $A^2 \rightarrow P^3$ reaction is not linked to proton uptake or release from solution. In the next step, a proton is taken up through the D pathway forming state F^3 with a time constant of ~100 μs (at pH 7.6). At the same time, the electron at Cu_A equilibrates with heme *a* (see Figure 1b). In the last step, the electron distributed between Cu_A and heme *a* is transferred to the catalytic site forming the oxidized Cyt*c*O in state O^4 (or O^0). Both the $P^3 \rightarrow F^3$ and $F^3 \rightarrow O^4$ transitions are each linked to pumping of one proton across the membrane (Figure 1b) (*17–19*).

Initial studies of voltage changes during the reaction outlined above showed that the $A^2 \rightarrow P^3$ transition ($\tau \cong 30$ μs) was not associated with any voltage changes (*17*), which is reasonable because the reaction involves electron transfer from heme *a* to the catalytic site, which takes place essentially parallel to the membrane surface (*1, 2*), and it is not linked to proton uptake from solution. The next two transitions, $P^3 \rightarrow F^3$ and $F^3 \rightarrow O^4$, involve electron transfer from Cu_A to heme *a*, proton transfer from solution to the catalytic site, and proton pumping across the membrane, and therefore, both these transitions give rise to large voltage changes (termed electrogenic events) (*17*). In a more recent study, Belevich et al. (*20*) found that also on the time scale of the $A^2 \rightarrow P^3$ transition ($\tau \cong 30$ μs) there is an electrogenic event within Cyt*c*O. At neutral pH, the corresponding voltage change was observed only in the D132N mutant Cyt*c*O in which proton uptake from solution on the time scale of the $P^3 \rightarrow F^3$ transition is blocked (*21*). The electrogenic event was also observed in wild-type Cyt*c*O, but only at high pH where the $A^2 \rightarrow P^3$ and $P^3 \rightarrow F^3$ transitions are well separated in time (*20*). Belevich et al. attributed the $A^2 \rightarrow P^3$ voltage change to an internal proton transfer from E286 to an unidentified acceptor for pumped protons, which would initiate the sequence of events leading to proton pumping (*20*).

The aim of this study was to further investigate the origin of the $A^2 \rightarrow P^3$ electrogenic events because identifying electron transfer reactions coupled to vectorial proton transfer is fundamental for understanding the proton pumping mechanism in Cyt*c*O. In an earlier study, we observed that the $A^2 \rightarrow P^3$ transition was slowed in structural variants of Cyt*c*O in which residues in the K pathway were modified (*22*) (see also ref *23*). The results suggested that the positively charged K362 side chain moves toward heme a_3 and Cu_B upon electron transfer to the catalytic site. In other words, electron transfer into the catalytic site could be electrogenic due to charge movement within the K pathway, which would contribute to the voltage changes observed by Belevich et al. (*20*), discussed above. To test this hypothesis, in this study we have investigated both voltage and absorbance changes upon reaction with O_2 of the fully reduced membrane-reconstituted wild-type Cyt*c*O and a structural variant in which Lys362 was replaced with a Met (K362M) (*24*). The electrometric measurements were also conducted in a mutant Cyt*c*O in which Ser299, located just below K362, was replaced with a Glu (S299E). The analogous S299D mutant Cyt*c*O displays qualitatively the same behavior as the K362M mutant Cyt*c*O, presumably because the K362 side chain is bound electrostatically to D299 (*22, 25*). Taken together, the

results from this study indicate that the voltage change, linked to electron transfer from heme *a* to the catalytic site, to a large extent originates from charge transfer within the K pathway.

MATERIALS AND METHODS

Purification of CytcO. Histidine-tagged Cyt*c*O was expressed in *R. sphaeroides* and purified as described in ref *26*. The S299E mutant of the *R. sphaeroides* Cyt*c*O was prepared as described in ref *24* (see also ref *27*). The K362M mutant strain was obtained from R. B. Gennis (*24*). Solubilized Cyt*c*O was purified using a His-tag nickel affinity column and eluted using 0.1 M imidazole, after which the buffer was exchanged for 0.1 M HEPES (pH 7.4) and 0.1% dodecyl β-D-maltoside. The enzyme was frozen in liquid nitrogen and stored at −80 °C.

Reconstitution of CytcO into SUVs. A lipid extract from soybean L-lecitin (Sigma, type II) was prepared by precipitation in acetone and then extraction in diethyl ether. The dried lipids were dissolved in a buffer containing 2% (w/v) cholate, 100 mM KCl, 25 mM HEPES (pH 7.6), 25 mM CAPS, and 100 μM EDTA. The solution was sonicated via two cycles of 30 s on and 30 s off per milliliter of lipid solution, using a tip sonicator (Sonicator Ultrasonic Processor XL2020, Heat Systems) under a N_2 atmosphere followed by a centrifugation step (4000 rpm for 20–40 min) to remove titanium particles.

Cyt*c*O, prepared as described above, was diluted in 4% (w/v) cholate, 100 mM KCl, 25 mM HEPES (pH 7.6), 25 mM CAPS, and 100 μM EDTA. Reconstitution of the enzyme into small unilamellar vesicle (SUVs) was done following a modified protocol from ref *17*, described in ref *19*. The diameter of the SUVs was ∼300 Å.

Flow-Flash Optical Absorption Measurements. The flow-flash technique was used to monitor the reaction of the four-electron reduced Cyt*c*O with O_2. The pH of the Cyt*c*O/SUV solution was adjusted to 7.6 or 10.5 (see figure legends), and the solution was transferred to an anaerobic cuvette in which the atmosphere was exchanged with N_2. Reduction of all four redox-active metal centers was achieved by anaerobic addition of 3 mM ascorbate and 1 μM hexaammineruthenium chloride. The reduction process was monitored on a Cary 400 Bio UV–visible spectrophotometer (Varian). Once reduction was complete, the atmosphere was exchanged with CO and binding of CO to the enzyme was confirmed by analysis of the absorption spectrum. Cyt*c*O SUVs were loaded anaerobically into a drive syringe of a modified stopped-flow apparatus and mixed 1:1 with an oxygen-saturated solution containing 100 mM KCl, 25 mM HEPES, 25 mM CAPS, and 100 μM EDTA at pH 7.6 or 10.5. Approximately 250 ms after mixing, the reaction was initiated by a short (∼8 ns) laser flash at 532 nm and the absorbance changes were monitored at specific wavelengths (see figure legends) over the course of ≤500 μs. In these measurements, a pulsed actinic light source was used as described in detail in ref *28*.

Voltage Changes across CytcO Oriented in Membranes. The electrometric setup used to measure voltage changes associated with charge movement across Cyt*c*O oriented in a membrane was essentially the same as that used by Verkhovsky, Wikström, and colleagues (*29*). The measuring cell consists of two 1 mL compartments separated by a Teflon film, covered by a lipid solution (in *n*-decane, 100 mg of soybean IIS lecithin/mL of *n*-decane). A solution containing Cyt*c*O SUVs in 0.1 M MOPS (pH 7.5) was added to one of the two cell compartments, and binding to the Teflon−lipid surface was initiated upon addition of 15 mM $CaCl_2$ and incubation for 2–3 h, after which both chambers were rinsed with buffer (a mixture of Bis-Tris propane, CHES, and CAPS each at 0.33 M) several times to remove unattached Cyt*c*O liposomes. The measuring cell was placed in an airtight chamber, and air was replaced consecutively by N_2 and then CO. To remove trace amounts of O_2 and reduce the Cyt*c*O, a solution containing 50 mM glucose, 0.12 mg/mL glucose oxidase, 75 μg/mL catalase, and 50 μM *N*,*N*,*N*′,*N*′-tetramethyl-*p*-phenylenediamine (TMPD) was added. For measurements at pH values other than that of the incubation buffer, experiments were conducted ∼1 h after the pH had been changed to allow the buffer on the inside of the Cyt*c*O liposomes to equilibrate with the outside solution. The reaction of the fully reduced Cyt*c*O with O_2 was initiated by injection of 50 μL of O_2-saturated buffer toward the Teflon film and ∼0.2 s after the addition the CO ligand was photolyzed with a laser flash. Voltage changes associated with charge transfer perpendicular to the membrane surface were measured using Ag/AgCl electrodes (DRIREF-2SH, World Precision Instruments) inserted into each of the compartments, i.e., on each side of the Teflon membrane. Because reduction of the K362M mutant Cyt*c*O is much slower than that of wild-type Cyt*c*O (*24, 30*) (we found that the mutant Cyt*c*O, reconstituted in SUVs, was fully reduced after 3–5 h at pH 7.6), the enzyme was allowed to be reduced overnight at room temperature in the dark. Care was exercised to make sure that the sample was kept in the dark until the first measurement.

To test the stability of the enzyme at high pH, we performed an experiment in which data were first recorded at pH 11 and then the pH was lowered to 8.5. In this experiment, the data at pH 8.5 were the same as those collected with the enzyme that was initially equilibrated with a pH 8.5 buffer.

RESULTS

In the experiments described below, the reaction of the fully reduced Cyt*c*O with O_2 was investigated. The reduced enzyme with the blocking CO ligand, bound to heme a_3, was mixed with an O_2-saturated solution. Approximately 0.2 s after mixing, the CO ligand was removed by a short laser flash, after which O_2 was bound to heme a_3. Progressive oxidation of the reduced enzyme was followed in time by measuring both absorbance changes associated with redox changes of the metal sites and voltage changes across Cyt*c*O oriented in a membrane.

Absorbance Changes Associated with CytcO Oxidation. Figure 2 shows absorbance changes at 595 nm for wild-type and K362M mutant Cyt*c*O, reconstituted in lipid vesicles, at pH 7.6 and 10.5 (same pH on both sides of the membrane). At this wavelength, it is possible to observe O_2 binding and formation of the P^3 state at the catalytic site (*20*). Experiments were conducted in membrane-reconstituted Cyt*c*O to maintain conditions similar to those used in the electrometric studies (see below). The initial decrease in absorbance at time zero is associated with flash-induced dissociation of the

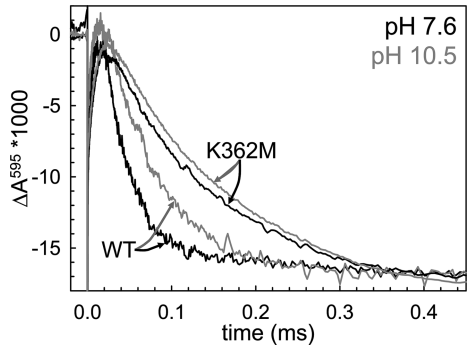

FIGURE 2: Absorbance changes at 595 nm during reaction with O_2 of fully reduced wild-type and K362M Cyt*c*O, reconstituted in SUVs. The decrease in absorbance at time zero is due to CO dissociation. The following increase and decrease in absorbance are associated with formation of the A^2 ($R^2 \rightarrow A^2$) and P^3 ($A^2 \rightarrow P^3$) states, respectively. At pH 7.6 (black traces), the $A^2 \rightarrow P^3$ transition displayed time constants of ~30 and 90 μs for wild-type (WT) and K362M mutant Cyt*c*O, respectively. At pH 10.5 (gray traces), the time constants were 70 and 100 μs for wild-type and K362M mutant Cyt*c*O, respectively. For these experiments, Cyt*c*O-containing SUVs were mixed 1:1 with an oxygen-saturated buffer. Concentrations after mixing were as follows: 100 mM KCl, 25 mM HEPES (pH 7.6), 25 mM CAPS (pH 10.5), 100 μM EDTA, 0.5 mM O_2, 1.5 mM ascorbate, and 0.5 mM hexaammineruthenium chloride.

CO ligand. The increase in absorbance with a time constant of ~10 μs originates from O_2 binding to reduced heme a_3, i.e., formation of state A^2 (at 0.5 mM O_2, i.e., O_2 binding is faster than with detergent-solubilized Cyt*c*O). The slower decrease in absorbance is associated with the $A^2 \rightarrow P^3$ transition. With wild-type Cyt*c*O at pH 7.6 (black trace) and pH 10.5 (gray trace), this transition displayed time constants of ~30 and ~70 μs, respectively. With the K362M mutant Cyt*c*O, the transition was slower: ~90 μs (black trace) and ~100 μs (gray trace) at pH 7.6 and 10.5, respectively.

The rates of the $P^3 \rightarrow F^3$ and $F^3 \rightarrow O^4$ transitions in wild-type Cyt*c*O have been measured over a broad pH range (*31, 32*), and that of the K362M mutant Cyt*c*O has been determined at neutral pH (*23, 25*). These rates are given in Table 1. In this study, we also determined the $F^3 \rightarrow O^4$ transition rate at pH 10.5 with the K362M mutant Cyt*c*O, and it is also given in Table 1.

Voltage Changes Associated with CytcO Oxidation. Figure 3 shows voltage changes upon reaction of the fully reduced Cyt*c*O with O_2. Figure 3a shows the development of the membrane potential for wild-type (black trace) and K362M Cyt*c*Os (gray trace) at pH 7.5. After an electrically silent period (lag phase, $\tau \cong 55$ μs), the membrane potential developed in three kinetic phases with time constants of 220 μs (59%), 0.86 ms (25%), and 3.8 ms (16%) (relative amplitudes in parentheses) for wild-type Cyt*c*O. With the K362M mutant Cyt*c*O, the total voltage change was similar to that observed with wild-type Cyt*c*O (*18*), and the time constants (amplitudes) were 60 μs for the lag phase and 330 μs (66%), 1.1 ms (24%), and 4.0 ms (10%) for the three following phases respectively.

At pH 10.5 (Figure 3b), the membrane potential also developed in three phases for wild-type Cyt*c*O (black trace), with time constants of 110 μs (53%), 1.3 ms (17%), and 14 ms (30%), while only two phases could be observed with the K362M mutant Cyt*c*O (gray trace), with time constants of 1.3 ms (55%) and 12 ms (45%). In other words, the rapid 100 μs component, seen with wild-type Cyt*c*O at pH 10.5, was not observed with the K362M mutant Cyt*c*O. For wild-type Cyt*c*O at pH 10.5, the initial lag phase was 30 μs, i.e., shorter than at pH 7.5. For the K362M mutant Cyt*c*O, the lag was much longer, 95 μs. Figure 4 shows a comparison of the initial kinetic phases measured at pH 10.5 with wild-type and K362M mutant Cyt*c*Os.

The results from the electrometric measurements with the S299E mutant enzyme (data not shown) were essentially identical to those obtained with the K362M mutant; i.e., the rapid electrogenic event observed in the wild-type enzyme at pH 10.5 was not present.

DISCUSSION

First, we note that even though the experiments in this study were performed with Cyt*c*O from *R. sphaeroides* while those presented by Wikström and colleagues (*20*) were done with *Paracoccus denitrificans* Cyt*c*O, the results were qualitatively the same. In addition, we repeated their experiments with the D132N mutant Cyt*c*O (not shown; see the introductory section and ref *20*) and obtained the same results. Thus, even though differences between the *P. denitrificans* and *R. sphaeroides* Cyt*c*Os have been reported previously (see, e.g., ref *33*), the results discussed above show that the electrogenic events proposed by Belevich et al. (*20*) to be linked to the $A^2 \rightarrow P^3$ transition are not unique for the *P. denitrificans* enzyme.

At pH 7.6, the $A^2 \rightarrow P^3$ transition with wild-type Cyt*c*O, determined from the absorbance changes, displayed a time constant of ~30 μs (Figure 2) which is in agreement with previous results (*12, 34–36*). At this pH, the $P^3 \rightarrow F^3$ and $F^3 \rightarrow O^4$ transitions display time constants of ~100 μs and ~1.5 ms, respectively, in detergent solution (*12, 17, 37*). In the electrometric measurements at pH 7.5 (Figure 3a), first a lag phase was observed, presumably corresponding to the $A^2 \rightarrow P^3$ transition (*17*). It was followed by three kinetic phases with time constants of 220 μs, attributed to the $P^3 \rightarrow F^3$ transition (~60% of the total amplitude) and a biphasic $F^3 \rightarrow O^4$ transition with time constants of 0.86 and 3.8 ms. A biphasic $F^3 \rightarrow O^4$ transition has been observed previously (*17, 38*).

With the K362M mutant Cyt*c*O at pH 7.6, the $A^2 \rightarrow P^3$ transition, determined from the absorbance changes, was slower and displayed a time constant of ~90 μs (Figure 2). Also in this case, a lag ($\tau \cong 60$ μs) was observed in the electrometric measurements and then the voltage developed in three kinetic phases with time constants of 330 μs ($P^3 \rightarrow F^3$, 66% of the total amplitude) and 1.1 and 4.0 ms, i.e., similar to those observed with wild-type Cyt*c*O. A slower $A^2 \rightarrow P^3$ transition with the K362M mutant than with wild-type Cyt*c*O was noted previously (*23*), and it was attributed to the removal of the positively charged K362 residue (*22, 25*) (see the more detailed discussion below).

With wild-type Cyt*c*O at pH 10.5, the $A^2 \rightarrow P^3$ transition (absorbance changes at 595 nm) was slightly slower than at pH 7.6 and displayed a time constant of ~70 μs (~30 μs at pH 7.6) (Figure 2). Such a weak pH dependence of the $A^2 \rightarrow P^3$ transition has been observed previously with the mitochondrial Cyt*c*O from bovine heart (*36*). The slightly slower $A^2 \rightarrow P^3$ transition may be due to titration of K362, which due to less positive charge at high pH would destabilize the negative charge at the catalytic site. This

Table 1: Time Constants for the Transitions in the Voltage and Absorbance Changes Measured with Wild-Type (WT), K362M, and S299E Cyt*c*Os[a]

		voltage change (ΔV)				absorbance change (ΔA)		
		τ_{lag} (μs)	τ_1 (μs)	τ_2 (ms)	τ_3 (ms)	$\tau(A^2 \rightarrow P^3)$ (μs)	$\tau(P^3 \rightarrow F^3)$ (μs)	$\tau(F^3 \rightarrow O^4)$ (ms)
pH 7.5/7.6	WT	55 ± 3	220 ± 14 ($59 \pm 1\%$)	0.86 ± 0.05 ($25 \pm 1\%$)	3.8 ± 0.3 ($16 \pm 1\%$)	30	100–130 (*12, 31*)	1.3–1.6 (*12,32*)
	K362M	60 ± 8	330 ± 30 ($66 \pm 3\%$)	1.1 ± 0.2 ($24 \pm 2\%$)	4.0 ± 1 ($10 \pm 3\%$)	90	130 (*25*)	~1.5 (*25*)
	S299E	57 ± 4	390 ± 11	1.2 ± 1	3.6 ± 0.5		130	1.1 (*22*)
pH 10.5	WT	30 ± 5	110 ± 5 ($53 \pm 3\%$)	1.3 ± 0.1 ($17 \pm 4\%$)	14 ± 3 ($30 \pm 3\%$)	70	(1.4 ms at pH 10.25) (*31*)	10 (*32*)
	K362M	95 ± 5	ND[b]	1.3 ± 0.2 ($55 \pm 5\%$)	12 ± 2 ($45 \pm 5\%$)	100	ND[b]	10–20
	S299E	88 ± 3	ND[b]	0.7 ± 0.1	5.0 ± 0.2	–[c]	–[c]	–[c]

[a] For the voltage changes, the standard errors are based on measurements on three separate samples (relative amplitudes given in parentheses). The $A^2 \rightarrow P^3$ transition rate and the $F^3 \rightarrow O^4$ transition rate with the K362M mutant Cyt*c*O were determined in this study from measurements on membrane-reconstituted Cyt*c*O (errors in the rates of <10%). The remaining data were taken from the literature (see references). [b] Not detected. [c] Absorbance changes with the S299E mutant Cyt*c*O at pH 10.5 were not measured.

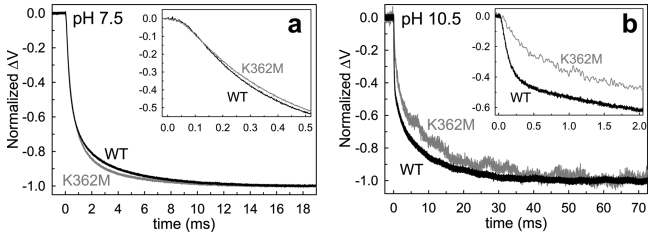

FIGURE 3: Generation of membrane potential during reaction of O_2 with fully reduced wild-type (WT) (black traces) and K362M (gray traces) Cyt*c*O, reconstituted in SUVs at pH 7.5 (a) and 10.5 (b). In panels a and b, the insets show the first 0.5 and 2.0 ms, respectively. The time constants of the transitions are given in Table 1. Experiments were conducted in 0.1 M buffer (equal amounts of Bis-Tris propane, CHES, and CAPS), 50 mM glucose, 0.12 mg/mL glucose oxidase, 75 μg/mL catalase, and 50 μM TMPD. A volume of 50 μL of O_2-saturated buffer was injected at the Teflon membrane 0.2 s before the reaction was initiated by flash photolysis of the CO ligand. For more details, see Materials and Methods. The data were normalized such that the difference between the voltage at the end of the reaction and at time 0 was set to 1 (*20*). The normalization could be done because the wild-type and K362M mutant Cyt*c*Os react to the same extent at a specific pH (*22, 23, 25*).

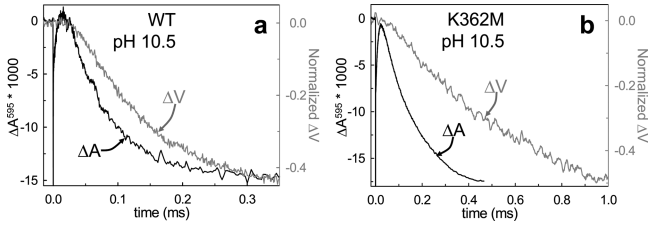

FIGURE 4: Absorbance changes at 595 nm (ΔA_{595}) and membrane potential generation (ΔV) during reaction with O_2 of fully reduced wild-type (WT) (a) and K362M mutant (b) Cyt*c*O at pH 10.5. The decrease in absorbance (black traces) is associated with the $A^2 \rightarrow P^3$ transition. With wild-type Cyt*c*O, the absorbance and voltage changes displayed similar time constants (~70 and ~110 μs, respectively) (panel a). With the K362M mutant Cyt*c*O, the voltage change was significantly slower (~1.3 ms) than the absorbance change (~100 μs) (panel b). Data were extracted from Figures 2 and 3.

explanation is consistent with the slower $A^2 \rightarrow P^3$ transition with the K362M mutant Cyt*c*O and the similar rates at pH 7.6 ($\tau \cong 90$ μs) and pH 10.5 ($\tau \cong 100$ μs) with this mutant Cyt*c*O.

At high pH, the $P^3 \rightarrow F^3$ and $F^3 \rightarrow O^4$ transitions are slowed because they are linked to proton uptake from solution (*12*). Results from previous studies with wild-type Cyt*c*O have shown that the rates of these reactions are pH-dependent such that at pH 10.25 the $P^3 \rightarrow F^3$ time constant is ~1.4 ms (the transient could not be resolved at higher pH), while the $F^3 \rightarrow O^4$ transition displays a time constant of ~10 ms at pH 10.5 (*31, 32*). As seen in Figure 3b and also observed previously (*20*), a voltage change with a time constant of ~110 μs and an amplitude of ~53% of the total voltage change was observed with wild-type Cyt*c*O at pH 10.5. This voltage change is significantly faster than the $P^3 \rightarrow F^3$ transition at high pH ($\tau > 1.4$ ms, determined from absorbance changes), i.e., the first transition that is associated with proton uptake from solution. Instead, the 110 μs voltage change approximately coincides in time with the $A^2 \rightarrow P^3$ transition, i.e., electron transfer from heme *a* to the catalytic site ($\tau \cong 70$ μs) (see Figure 4a).

The difference in time constants of the absorbance change attributed to the $A^2 \rightarrow P^3$ transition ($\tau \cong 70$ μs) and the 110 μs voltage change, proposed to originate from the same reaction, may be due to slightly different experimental conditions (for example, in the electrometric measurements Ca^{2+} is added to the Cyt*c*O/SUV solution and the SUVs are attached to a surface). Alternatively, if the difference in time constants would indeed be significant, then the results would indicate that the voltage change follows after the $A^2 \rightarrow P^3$ transition, which would further strengthen the general conclusions of this study (see below).

With the K362M mutant Cyt*c*O at pH 10.5, the $A^2 \rightarrow P^3$ transition displayed a time constant of ~100 μs (see Figure 2); however, no voltage changes were observed on the time scale of this transition (Figure 4b), and a lag phase with a time constant of ~95 μs was followed by voltage changes with time constants of ~1.3 ms and ~12 ms.

Because with the K362M mutant Cyt*c*O the $A^2 \rightarrow P^3$ transition is not associated with any voltage changes (Figure 4b), we propose that the voltage change observed at high pH with wild-type Cyt*c*O (Figure 4a) is related to charge transfer within the K pathway. Some contribution to the $A^2 \rightarrow P^3$ voltage change from charge movement within the K pathway has also been suggested previously (*39*).

A relevant question is the origin of this charge transfer within the K pathway. As already noted above, the $A^2 \rightarrow P^3$ transition is not associated with proton uptake from solution. Thus, the charge transfer must take place within Cyt*c*O. A role for the K pathway in charge compensation has been proposed previously by Rich and colleagues, who suggested that charge displacement within the pathway may stabilize changes in charge at the catalytic site (*40*). One possibility is that this charge compensation is achieved through movement of the positively charged K362 side chain upon electron

transfer to the catalytic site (ref *22*; see also ref *41*). This conclusion would be supported by the slowed $A^2 \rightarrow P^3$ transition at high pH with wild-type Cyt*c*O and also a slowed and essentially pH independent $A^2 \rightarrow P^3$ transition observed with the K362M mutant Cyt*c*O. Even though results from some electrostatic calculations indicate that the K362 side chain is not charged (*42, 43*), when a water molecule near K362 is included in such calculations (as proposed in ref *22*), the K362 pK_a increases such that the side chain is 50% charged up to pH ~11.2 (*39*).

As outlined above, the results obtained with wild-type Cyt*c*O are qualitatively the same as those presented in ref *20*. However, our interpretation is different, based on our new results with the K362M mutant Cyt*c*O. The proposal that the 110 μs electrogenic reaction, simultaneous with the $A^2 \rightarrow P^3$ transition at high pH, is due to internal proton transfer from Glu286 to an acceptor site for pumped protons (*20*) mainly rests on the observation that the voltage change was not observed [or it was very small (*39*)] with the E286Q mutant Cyt*c*O. In this mutant Cyt*c*O, upon reaction of the fully reduced Cyt*c*O with O_2, the P^3 state is formed but the remaining part of the reaction is completely blocked, and there are no electron transfers perpendicular to the membrane or proton uptake from solution (*44*). If the $A^2 \rightarrow P^3$ voltage change originates from charge movement within the K pathway, we would expect this voltage change to remain in the E286Q mutant Cyt*c*O. However, because no other voltage changes are expected to be seen in the E286Q mutant Cyt*c*O, it would be difficult to relate such a putative signal to other electrogenic events in Cyt*c*O. Also, in this mutant Cyt*c*O, the enzyme population with CO bound to heme a_3 is smaller than that in wild-type Cyt*c*O (*45*), which would reduce a putative voltage change in the E286Q mutant Cyt*c*O because <100% of the enzyme population would react with O_2.

The 110 μs voltage change observed with wild-type Cyt*c*O at high pH may seemingly appear very large (53% of the total voltage change) considering that it corresponds to charge transfer only within the K pathway. However, at pH 10.5, the Cyt*c*O presumably does not pump protons (H. Lepp et al., unpublished results, and ref *46*) and the net proton uptake upon oxidation is smaller (~1 H^+) than at neutral pH (~2 H^+) (*47*). Therefore, the number of charges transferred during the 110 μs voltage change is relatively small and would comprise only 15% of the total voltage change at neutral pH (*20*).

Earlier studies showed that reduction of the oxidized catalytic site, prior to O_2 binding, in K pathway mutants of Cyt*c*O was dramatically slowed, which was interpreted in terms of blocked proton uptake through the K pathway (*23, 30, 40, 48–51*). Furthermore, studies of internal electron transfer between hemes *a* and a_3 in the absence of O_2 showed that reduction and oxidation of heme a_3 are linked to proton uptake and release, respectively, through the K pathway (*25, 52, 53*), yet after the catalytic site is reduced and O_2 is bound to heme a_3, the K pathway is not used for proton transfer and all protons, both those used for O_2 reduction and those that are pumped, are transferred through the D pathway (*48–51*). An important question is what prevents protons from being transferred through the K pathway after binding of O_2 (see also the discussion in ref *6*). It is possible that the electrogenic structural change within the pathway, discussed in this work, may close the pathway for further proton transfer during O_2 reduction.

ACKNOWLEDGMENT

We thank Dr. Michael Verkhovsky for invaluable help with the setup for electrometric measurements. The project was supported by grants from the Swedish Research Council and the Knut and Alice Wallenberg Foundation.

REFERENCES

1. Svensson-Ek, M., Abramson, J., Larsson, G., Törnroth, S., Brzezinski, P., and Iwata, S. (2002) The X-ray Crystal Structures of Wild-Type and EQ(I-286) Mutant Cytochrome *c* Oxidases from *Rhodobacter sphaeroides*. *J. Mol. Biol. 321*, 329–339.
2. Qin, L., Hiser, C., Mulichak, A., Garavito, R. M., and Ferguson-Miller, S. (2006) Identification of conserved lipid/detergent-binding sites in a high-resolution structure of the membrane protein cytochrome c oxidase. *Proc. Natl. Acad. Sci. U.S.A. 103*, 16117–16122.
3. Brändén, G., Gennis, R. B., and Brzezinski, P. (2006) Transmembrane proton translocation by cytochrome *c* oxidase. *Biochim. Biophys. Acta 1757*, 1052–1063.
4. Brzezinski, P., and Ädelroth, P. (2006) Design principles of proton-pumping haem-copper oxidases. *Curr. Opin. Struct. Biol. 16*, 465–472.
5. Gennis, R. B. (2004) Coupled proton and electron transfer reactions in cytochrome oxidase. *Front. Biosci. 9*, 581–591.
6. Wikström, M., and Verkhovsky, M. I. (2007) Mechanism and energetics of proton translocation by the respiratory heme-copper oxidases. *Biochim. Biophys. Acta 1767*, 1200–1214.
7. Hosler, J. P., Ferguson-Miller, S., and Mills, D. A. (2006) Energy transduction: Proton transfer through the respiratory complexes. *Annu. Rev. Biochem. 75*, 165–187.
8. Mills, D. A., and Ferguson-Miller, S. (2003) Understanding the mechanism of proton movement linked to oxygen reduction in cytochrome c oxidase: Lessons from other proteins. *FEBS Lett. 545*, 47–51.
9. Papa, S., Capitanio, G., and Luca Martino, P. (2006) Concerted involvement of cooperative proton-electron linkage and water production in the proton pump of cytochrome c oxidase. *Biochim. Biophys. Acta 1757*, 1133–1143.
10. Brunori, M., Giuffre, A., and Sarti, P. (2005) Cytochrome c oxidase, ligands and electrons. *J. Inorg. Biochem. 99*, 324–336.
11. Richter, O. M., and Ludwig, B. (2003) Cytochrome c oxidase: Structure, function, and physiology of a redox-driven molecular machine. *Rev. Physiol. Biochem. Pharmacol. 147*, 47–74.
12. Ädelroth, P., Ek, M., and Brzezinski, P. (1998) Factors Determining Electron-Transfer Rates in Cytochrome *c* Oxidase: Investigation of the Oxygen Reaction in the *R. sphaeroide*s and Bovine Enzymes. *Biochim. Biophys. Acta 1367*, 107–117.
13. Ferguson-Miller, S., and Babcock, G. T. (1996) Heme/copper terminal oxidases. *Chem. Rev. 96*, 2889–2907.
14. Brzezinski, P. (2004) Redox-driven membrane-bound proton pumps. *Trends Biochem. Sci. 29*, 380–387.
15. Babcock, G. T., and Wikström, M. (1992) Oxygen activation and the conservation of energy in cell respiration. *Nature 356*, 301–309.
16. Einarsdóttir, Ó., and Szundi, I. (2004) Time-resolved optical absorption studies of cytochrome oxidase dynamics. *Biochim. Biophys. Acta 1655*, 263–273.
17. Jasaitis, A., Verkhovsky, M. I., Morgan, J. E., Verkhovskaya, M. L., and Wikström, M. (1999) Assignment and charge translocation stoichiometries of the major electrogenic phases in the reaction of cytochrome c oxidase with dioxygen. *Biochemistry 38*, 2697–2706.
18. Bloch, D., Belevich, I., Jasaitis, A., Ribacka, C., Puustinen, A., Verkhovsky, M. I., and Wikström, M. (2004) The catalytic cycle of cytochrome c oxidase is not the sum of its two halves. *Proc. Natl. Acad. Sci. U.S.A. 101*, 529–533.
19. Faxén, K., Gilderson, G., Ädelroth, P., and Brzezinski, P. (2005) A mechanistic principle for proton pumping by cytochrome c oxidase. *Nature 437*, 286–289.
20. Belevich, I., Verkhovsky, M. I., and Wikström, M. (2006) Proton-coupled electron transfer drives the proton pump of cytochrome c oxidase. *Nature 440*, 829–832.

21. Smirnova, I. A., Ädelroth, P., Gennis, R. B., and Brzezinski, P. (1999) Aspartate-132 in cytochrome c oxidase from *Rhodobacter sphaeroides* is involved in a two-step proton transfer during oxo-ferryl formation. *Biochemistry 38*, 6826–6833.
22. Brändén, M., Sigurdson, H., Namslauer, A., Gennis, R. B., Ädelroth, P., and Brzezinski, P. (2001) On the role of the K-proton transfer pathway in cytochrome c oxidase. *Proc. Natl. Acad. Sci. U.S.A. 98*, 5013–5018.
23. Ädelroth, P., Gennis, R. B., and Brzezinski, P. (1998) Role of the pathway through K(I-362) in proton transfer in cytochrome c oxidase from *R. sphaeroides*. *Biochemistry 37*, 2470–2476.
24. Hosler, J. P., Shapleigh, J. P., Mitchell, D. M., Kim, Y., Pressler, M. A., Georgiou, C., Babcock, G. T., Alben, J. O., Ferguson-Miller, S., and Gennis, R. B. (1996) Polar residues in helix VIII of subunit I of cytochrome c oxidase influence the activity and the structure of the active site. *Biochemistry 35*, 10776–10783.
25. Brändén, M., Tomson, F., Gennis, R. B., and Brzezinski, P. (2002) The entry point of the K-proton-transfer pathway in cytochrome c oxidase. *Biochemistry 41*, 10794–10798.
26. Zhen, Y., Qian, J., Follmann, K., Hosler, J., Hayward, T., Nilsson, T., Dahn, M., Hilmi, Y., Hamer, A., Hosler, J., and Ferguson-Miller, S. (1998) Overexpression and purification of cytochrome coxidase from *Rhodobacter sphaeroides*. *Protein Expression Purif. 13*, 326–336.
27. Aagaard, A., Gilderson, G., Mills, D. A., Ferguson-Miller, S., and Brzezinski, P. (2000) Redesign of the proton-pumping machinery of cytochrome c oxidase: Proton pumping does not require Glu(I-286). *Biochemistry 39*, 15847–15850.
28. Namslauer, A., Brändén, M., and Brzezinski, P. (2002) The rate of internal heme-heme electron transfer in cytochrome c oxidase. *Biochemistry 41*, 10369–10374.
29. Verkhovsky, M. I., Morgan, J. E., Verkhovskaya, M. L., and Wikström, M. (1997) Translocation of electrical charge during a single turnover of cytochrome-c oxidase. *Biochim. Biophys. Acta 1318*, 6–10.
30. Vygodina, T. V., Pecoraro, C., Mitchell, D., Gennis, R., and Konstantinov, A. A. (1998) Mechanism of inhibition of electron transfer by amino acid replacement K362M in a proton channel of *Rhodobacter sphaeroides* cytochrome c oxidase. *Biochemistry 37*, 3053–3061.
31. Namslauer, A., Aagaard, A., Katsonouri, A., and Brzezinski, P. (2003) Intramolecular proton-transfer reactions in a membrane-bound proton pump: The effect of pH on the peroxy to ferryl transition in cytochrome c oxidase. *Biochemsitry 42*, 1488–1498.
32. Brändén, G., Brändén, M., Schmidt, B., Mills, D. A., Ferguson-Miller, S., and Brzezinski, P. (2005) The protonation state of a heme propionate controls electron transfer in cytochrome c oxidase. *Biochemistry 44*, 10466–10474.
33. Richter, O.-M. H., Dürr, K. L., Ludwig, B., Kannt, A., Scandurra, F. M., Giuffrè, A., Sarti, P., and Hellwig, P. (2005) Probing the access of protons to the K pathway in the *Paracoccus denitrificans* cytochrome c oxidase. *FEBS J. 272*, 404–412.
34. Verkhovsky, M. I., Morgan, J. E., and Wikström, M. (1994) Oxygen binding and activation: Early steps in the reaction of oxygen with cytochrome c oxidase. *Biochemistry 33*, 3079–3086.
35. Hill, B. C. (1991) The reaction of the electrostatic cytochrome c-cytochrome oxidase complex with oxygen. *J. Biol. Chem. 266*, 2219–2226.
36. Oliveberg, M., Brzezinski, P., and Malmström, B. G. (1989) The effect of pH and temperature on the reaction of fully reduced and mixed-valence cytochrome c oxidase with dioxygen. *Biochim. Biophys. Acta 977*, 322–328.
37. Paula, S., Sucheta, A., Szundi, I., and Einarsdóttir, Ó. (1999) Proton and electron transfer during the reduction of molecular oxygen by fully reduced cytochrome c oxidase: A flow-flash investigation using optical multichannel detection. *Biochemistry 38*, 3025–3033.
38. Siletsky, S. A., Pawate, A. S., Weiss, K., Gennis, R. B., and Konstantinov, A. A. (2004) Transmembrane charge separation during the ferryl-oxo → oxidized transition in a nonpumping mutant of cytochrome c oxidase. *J. Biol. Chem. 279*, 52558–52565.
39. Tuukkanen, A., Verkhovsky, M. I., Laakkonen, L., and Wikström, M. (2006) The K-pathway revisited: A computational study on cytochrome c oxidase. *Biochim. Biophys. Acta 1757*, 1117–1121.
40. Jünemann, S., Meunier, B., Gennis, R. B., and Rich, P. R. (1997) Effects of mutation of the conserved lysine-362 in cytochrome c oxidase from *Rhodobacter sphaeroides*. *Biochemistry 36*, 14456–14464.
41. Hofacker, I., and Schulten, K. (1998) Oxygen and proton pathways in cytochrome c oxidase. *Proteins 30*, 100–107.
42. Popovic, D. M., and Stuchebrukhov, A. A. (2004) Electrostatic study of the proton pumping mechanism in bovine heart cytochrome c oxidase. *J. Am. Chem. Soc. 126*, 1858–1871.
43. Kannt, A., Roy, C., Lancaster, D., and Michel, H. (1998) The coupling of electron transfer and proton translocation: Electrostatic calculations on *Paracoccus denitrificans* cytochrome c oxidase. *Biophys. J. 74*, 708–721.
44. Ädelroth, P., Svensson Ek, M., Mitchell, D. M., Gennis, R. B., and Brzezinski, P. (1997) Glutamate 286 in cytochrome aa3 from *Rhodobacter sphaeroides* is involved in proton uptake during the reaction of the fully-reduced enzyme with dioxygen. *Biochemistry 36*, 13824–13829.
45. Jünemann, S., Meunier, B., Fisher, N., and Rich, P. R. (1999) Effects of mutation of the conserved glutamic acid-286 in subunit I of cytochrome c oxidase from *Rhodobacter sphaeroides*. *Biochemistry 38*, 5248–5255.
46. Verkhovskaya, M., Verkhovsky, M., and Wikström, M. (1992) pH dependence of proton translocation by *Escherichia coli*. *J. Biol. Chem. 267*, 14559–14562.
47. Hallén, S., and Nilsson, T. (1992) Proton transfer during the reaction between fully reduced cytochrome c oxidase and dioxygen: pH and deuterium isotope effects. *Biochemistry 31*, 11853–11859.
48. Konstantinov, A. A., Siletsky, S., Mitchell, D., Kaulen, A., and Gennis, R. B. (1997) The roles of the two proton input channels in cytochrome c oxidase from *Rhodobacter sphaeroides* probed by the effects of site-directed mutations on time-resolved electrogenic intraprotein proton transfer. *Proc. Natl. Acad. Sci. U.S.A. 94*, 9085–9090.
49. Pecoraro, C., Gennis, R. B., Vygodina, T. V., and Konstantinov, A. A. (2001) Role of the K-channel in the pH-dependence of the reaction of cytochrome c oxidase with hydrogen peroxide. *Biochemistry 40*, 9695–9708.
50. Wikström, M., Jasaitis, A., Backgren, C., Puustinen, A., and Verkhovsky, M. I. (2000) The role of the D- and K-pathways of proton transfer in the function of the haem-copper oxidases. *Biochim. Biophys. Acta 1459*, 514–520.
51. Brzezinski, P., and Ädelroth, P. (1998) Pathways of proton transfer in cytochrome c oxidase. *J. Bioenerg. Biomembr. 30*, 99–107.
52. Brändén, M., Namslauer, A., Hansson, Ö., Aasa, R., and Brzezinski, P. (2003) Water-hydroxide exchange reactions at the catalytic site of heme-copper oxidases. *Biochemistry 42*, 13178–13184.
53. Sigurdson, H., Brändén, M., Namslauer, A., and Brzezinski, P. (2002) Ligand binding reveals protonation events at the active site of cytochrome c oxidase: Is the K-pathway used for the transfer of H^+ or OH^-? *J. Inorg. Biochem. 88*, 335–342.
54. Humphrey, W., Dalke, A., and Schulten, K. (1996) VMD: Visual molecular dynamics. *J. Mol. Graphics 14*, 33–38.

BI7024707